ELASTODYNAMIC GREEN'S TENSOR IN VERTICALLY TRANSVERSELY ISOTROPIC MEDIA

ZHAO LI and EVGENY M. CHESNOKOV

Department of Earth and Atmospheric Sciences, University of Houston, Houston, TX 77004, U.S.A.
zli24@uh.edu; emchesno@central.uh.edu

(Received January 15, 2015; revised version accepted April 19, 2015)

ABSTRACT

Li, Z. and Chesnokov, E.M., 2015. Elastodynamic Green's tensor in vertically transversely isotropic media. *Journal of Seismic Exploration*, 24: 259-280.

The elastodynamic Green's tensor in a vertically transversely isotropic (VTI) medium is presented explicitly as an inverse Hankel transform. The asymptotic solution is found by the stationary phase approximation. An approximate formula in weak VTI media is derived based on a novel way of expanding the vertical slowness linearly to anisotropic parameters in which case the stationary-phase points can be found analytically. The approximate solution will become exact when the medium degenerates into an elliptical VTI rather than an isotropic medium.

KEY WORDS: anisotropy, Green's tensor, asymptotic, VTI, analytic solution.

INTRODUCTION

Transient elastic wave propagation in general anisotropic media has been studied extensively during the past century due to its theoretical significance as well as its application in seismology and related fields. The current work is dedicated to finding the elastodynamic Green's tensor in a vertically transversely isotropic medium.

Transversely isotropic (TI), or hexagonal, symmetry can be described by five independent elastic constants. One special type of TI symmetry is the VTI (vertically transversely isotropy) symmetry where the symmetric axis is located

0963-0651/15/$5.00

along the vertical axis. Due to the complexity of the calculation, most of the computational work is done numerically (for example: Dellinger, 1991; Hung and Forsyth, 1998). Analytic works on Green's tensor thus far have been focused on the asymptotic solution. One way to evaluate the asymptotic Green's tensor is by ray approximation (Gajewski, 1993). Vavryčuk (1997) found the analytic Green's tensor in weak-TI media by perturbing elastic constants from the isotropic medium. However, for the general TI media, the ray theory Green's tensor needs special treatment in the region close to shear-wave singularities (Gridin, 2000; Tsvankin, 2001; Vavryčuk, 2002).

A more conventional way of calculating Green's tensor is finding its image in other domains then transforming the solution back to the time-space domain. The method described in Tsvankin and Chesnokov (1990) is applied in the current work to find the analytic Green's tensor in VTI media. Green's tensor in frequency-slowness or plane-wave domain is derived explicitly and separated into a P-SV coupled term and a SH-wave term, in which case the solution would not be affected by shear-wave singularities. Then the inverse Fourier transform is evaluated in the cylindrical coordinate system and reduced to an inverse Hankel transform over horizontal slowness. The full waveform response in the frequency-space domain can be found by computing the inverse Hankel transform numerically. Such a solution can be extended to modeling the wave propagation in layered anisotropic media by the reflectivity method (Fuchs and Müller, 1972; Kennett, 1982; Müller, 1985).

Stationary phase approximation is being employed to evaluate Green's tensor in the asymptotic limit (high-frequency end in the current problem). The asymptotic SH-wave Green's tensor in a general VTI media can always be solved analytically (Vavryčuk, 1996) while the P-SV-part is much more complicated due to its physical nature. To the authors' knowledge, most of the existing analytical solutions yield a numerical calculation of the stationary-phase points (Tsvankin 1995) and these solutions are mostly sensitive to the degree of anisotropy, which can often be characterize by the value of anisotropic parameters (Thomsen, 1986). In the present paper, we propose a novel way of finding the approximate solution of P-SV Green's tensor in weak-TI media based on expanding the vertical slowness to the first-order of Thomsen parameters (Thomsen, 1986). Then the stationary-phase points can be found analytically by solving a set of cubic equations. This approximate solution is most accurate when the medium is close to elliptical anisotropy (Thomsen parameters $\delta = \varepsilon$) rather than isotropy.

The present paper is organized as follow: in section two, we review the procedure for solving Green's tensor described in Tsvankin and Chesnokov (1990). The asymptotic SH-wave Green's tensor is solved in the general VTI media and presented in section three. The approximate solution for weak-TI media is shown in section four. The approximate and numerically computed

results are compared (Appendix D) and the error introduced by the approximation is discussed. Throughout the current paper, the lower indices of a variable will vary from one to three. Einstein summation of repetitive lower indices is implied.

THE PROCEDURE FOR SOLVING THE GREEN'S TENSOR

In this section, we briefly review the method of calculating the Green's tensor, which is originally described in Tsvankin and Chesnokov (1990). The elastodynamic wave equation in homogeneous anisotropic media with a body force is shown in (1):

$$\rho(\partial^2 u_i/\partial t^2) = C_{ijkl}(\partial^2 u_k/\partial x_j \partial x_l) + f_i \quad , \tag{1}$$

where u_i is the i-th component of the displacement vector and f_i is the i-th component of the applied body force, ρ is the density and C_{ijkl} is the stiffness tensor of anisotropic media. In the present paper, C_{ijkl} is limited to VTI symmetry, which has five independent elements. Considering the symmetric property, C_{ijkl} can be shown as a second-rank tensor in (2):

$$C_{ij} = \begin{bmatrix} C_{11} & C_{12} & C_{13} & 0 & 0 & 0 \\ & C_{11} & C_{13} & 0 & 0 & 0 \\ & & C_{33} & 0 & 0 & 0 \\ & & & C_{44} & 0 & 0 \\ & & & & C_{44} & 0 \\ & & & & & C_{66} \end{bmatrix} , \tag{2}$$

$$C_{66} = (C_{11} - C_{12})/2 \quad ,$$

by Voigt notation. The displacement can be written in terms of the Green's tensor as (3)

$$u_i(r,t) = \int G_{ij}(\mathbf{r},\mathbf{r}_0;t,t_0) f_j(\mathbf{r}_0,t_0) d\mathbf{r}_0 dt_0 \quad , \tag{3}$$

and the body force can be projected by the delta function as (4)

$$f_i(r,t) = \int \delta(\mathbf{r} - \mathbf{r}_0)\delta(t - t_0) f_i(\mathbf{r}_0,t_0) d\mathbf{r}_0 dt_0 \quad , \tag{4}$$

where $\delta(x)$ is the Dirac-delta. For the purpose of being concise, we set the body force to be located at the origin ($\mathbf{r}_0$ and t_0 equal zero) and the Green's tensor can be simply written as $G_{ij}(\mathbf{r},t)$. Applying (3) and (4) into (1), the equation for Green's tensor can be found in (5)

$$[\rho\delta_{ik}(\partial^2/\partial t^2) - C_{ijkl}(\partial^2/\partial x_j \partial x_l)]G_{km}(\mathbf{r},t) = \delta_{im}\delta(\mathbf{r})\delta(t) \quad , \tag{5}$$

where δ_{ij} is the Kronecker-delta. In order to solve (5) analytically, we expand the Green's tensor and the Dirac-delta into Fourier series in (6)

$$\begin{aligned} G_{ij}(\mathbf{r},t) &= (1/2\pi) \int G_{ij}(\mathbf{p},\omega) e^{i\omega(t-\mathbf{p}\cdot\mathbf{r})} \omega^3 d\mathbf{p} d\omega \quad , \\ \delta(\mathbf{r})\delta(t) &= (1/2\pi) \int e^{i\omega(t-\mathbf{p}\cdot\mathbf{r})} \omega^3 d\mathbf{p} d\omega \quad , \end{aligned} \tag{6}$$

where $\mathbf{p}$ is the slowness vector and ω is the angular frequency. After applying (6), (5) will become (7)

$$\begin{aligned} L_{ik}G_{km}(\mathbf{k},\omega) &= -\delta_{im} \quad , \\ L_{ik} &= \omega^2(\rho\delta_{ik} - C_{ijkl}p_j p_l) \quad , \end{aligned} \tag{7}$$

and the Green's tensor can be found by calculating the inverse of L_{ik}. For VTI media, the solution in frequency-slowness domain is shown in (8)

$$\begin{aligned} G_{11} &= [-(\rho - C_{44}p_r^2 - C_{33}p_3^2)/\rho^2\omega^2(1 - p^2V_P^2)(1 - p^2V_{SV}^2)]\cos^2\varphi \\ &\quad - [1/\rho\omega^2(1 - p^2V_{SH}^2)]\sin^2\varphi \quad , \\ G_{22} &= -(\rho - C_{44}p_r^2 - C_{33}p_3^2)/\rho^2\omega^2(1 - p^2V_P^2)(1 - p^2V_{SV}^2)]\sin^2\varphi \\ &\quad - [1/\rho\omega^2(1 - p^2V_{SH}^2)]\cos^2\varphi \quad , \\ G_{33} &= -(\rho - C_{11}p_r^2 - C_{44}p_3^2)/\rho^2\omega^2(1 - p^2V_P^2)(1 - p^2V_{SV}^2) \\ G_{12} &= \{[-(\rho - C_{44}p_r^2 - C_{33}p_3^2)/\rho^2\omega^2(1 - p^2V_P^2)(1 - p^2V_{SV}^2)] \\ &\quad + [1/\rho\omega^2(1 - p^2V_{SH}^2)]\}\sin\varphi\cos\varphi \quad , \\ G_{13} &= -p_1p_3(C_{13} + C_{44})/\rho^2\omega^2(1 - p^2V_P^2)(1 - p^2V_{SV}^2) \quad , \\ G_{23} &= -p_2p_3(C_{13} + C_{44})/\rho^2\omega^2(1 - p^2V_P^2)(1 - p^2V_{SV}^2) \quad , \\ G_{31} &= G_{13} \quad , \quad G_{21} = G_{12} \quad , \quad G_{32} = G_{23} \quad . \end{aligned} \tag{8}$$

where p_1, p_2 and p_3 are components of the slowness vector in Cartesian coordinates. In cylindrical coordinates, the horizontal slowness p_r, azimuth angle image φ, polar angle image θ, and phase velocities of different modes (V_P, V_{SV}, and V_{SH}) are defined in (9)

$$\varphi = \tan^{-1}(p_2/p_1) \ ,$$

$$\theta = \tan^{-1}(p_3/p_r) \ ,$$

$$p_r = \sqrt{(p_1^2 + p_2^2)} \ ,$$

$$2\rho V_P^2 = (C_{11} + C_{44})\sin^2\theta + (C_{33} + C_{44})\cos^2\theta + K \ ,$$

$$2\rho V_{SV}^2 = (C_{11} + C_{44})\sin^2\theta + (C_{33} + C_{44})\cos^2\theta - K \ ,$$

$$\rho V_{SH}^2 = C_{66}\sin^2\theta + C_{44})\cos^2\theta \ ,$$

$$K = \sqrt{\{[(C_{11} - C_{44})\sin^2\theta - (C_{33} - C_{44})\cos^2\theta]^2 + 4(C_{13} + C_{44})^2\sin^2\theta\cos^2\theta\}} \ . \tag{9}$$

From (8), it can be seen that the Green's tensor is separated into two parts. One corresponds to the coupled P- and SV-wave motion, while the other to the SH-wave. The SH-wave Green's tensor is only related to the projection of the source's horizontal component, which reflects the property of the TI media. The P- SV- and SH-wave motions are separated in (8), which means that the simple shear-wave singularities will not affect future results.

In order to find the space-domain solution, the inverse Fourier transform in (6) needs to be computed. Considering the cylindrical coordinate system, we rewrite (6) into (10):

$$G_{ij}(r,z,\alpha,t) = [1/(2\pi)^4] \int_{-\infty}^{\infty}\int_{0}^{2\pi}\int_{-\infty}^{\infty}\int_{0}^{\infty} G_{ij}(p_r,p_3,\varphi,\omega) \times e^{i\omega[t-p_r r\cos(\varphi-\alpha)-p_3 z]}\, \omega^3 p_r dp_r dp_3 d\varphi d\omega \ , \tag{10}$$

where α is the spatial azimuth angle. The first integral over vertical slowness can be solved analytically by evaluating a contour integral and only the causal solution is considered in the present paper. Then (10) will become (11):

$$G_{ij}(r,z,\alpha,t) = [i/(2\pi)^3] \sum_{M=\alpha,\beta,\gamma} \int_{-\infty}^{\infty}\int_{0}^{2\pi}\int_{0}^{\infty} G_{ij}^{M}(p_r,z,\varphi,\omega) \times e^{i\omega[t-p_r r\cos(\varphi-\alpha)-p_M|z|]}\, \omega^3 p_r dp_r dp_3 d\varphi d\omega \ , \tag{11}$$

where p_M is the vertical slowness of different modes. They correspond to the propagation of three body-waves: p_α, p_β, and p_γ, for P-, SV-, and SH-wave, respectively. They are written explicitly in (12):

$$
\begin{aligned}
f &= 1 - (C_{44}/C_{33}) \ , \\
\varepsilon &= (C_{11} - C_{33})/2C_{33} \ , \\
\delta &= [(C_{13} + C_{44})^2 - (C_{33} - C_{44})^2]/2C_{33}(C_{33} - C_{44}) \ , \\
p_\alpha^2 &= [0.5/(f-1)][2(\varepsilon + 1 - f - f\delta)p_r^2 + (1/V_{P0}^2)(f-2) \\
&\quad + \sqrt{(\{4f^2[(\delta+1)^2 - 2\varepsilon - 1] + 8(\varepsilon - \delta - \varepsilon\delta)f + 4\varepsilon^2\}p_r^4} \\
&\quad + (8f\delta - 4f\varepsilon - 4f^2\delta)(p_r^2/V_{P0}^2)(f^2/V_{P0}^4))] \ , \\
p_\beta^2 &= [0.5/(f-1)][2(\varepsilon + 1 - f - f\delta)p_r^2 + (1/V_{P0}^2)(f-2) \\
&\quad - \sqrt{(\{4f^2[(\delta+1)^2 - 2\varepsilon - 1] + 8(\varepsilon - \delta - \varepsilon\delta)f + 4\varepsilon^2\}p_r^4} \\
&\quad + (8f\delta - 4f\varepsilon - 4f^2\delta)(p_r^2/V_{P0}^2)(f^2/V_{P0}^4))] \ , \\
p_\gamma^2 &= (1/V_{S0}^2) - (C_{66}/C_{44})p_r^2 \ , \\
V_{S0}^2 &= C_{44}/\rho \ , \quad V_{P0}^2 = C_{33}/\rho \ ,
\end{aligned}
\tag{12}
$$

with the anisotropic parameters ε and δ introduced by Thomsen (1986). The integral over the azimuth angle image φ in (11) can be carried out and replaced by Bessel functions. As can be seen from (8), the dependency of φ is only up to the second-order in the Green's tensor due to the rotational symmetry of VTI media. Then the Bessel integral can be calculated analytically. The result is shown in (13):

$$
\begin{aligned}
G_{ij}(r,z,\alpha,t) &= [i^{(l+1)}/(2\pi)^2] \sum_{l=0,1,2} \sum_{M=\alpha,\beta,\gamma} \int_{-\infty}^{\infty} \int_{0}^{\infty} G_{ij}^M(p_r,z,\alpha,\omega) \\
&\quad \times e^{i\omega(t - p_M|z|)} J_l(\omega p_r r)\omega^2 p_r dp_r d\omega \ ,
\end{aligned}
\tag{13}
$$

where $J_l(x)$ is the l-th order Bessel function of the first kind. The explicit formulas of G_{ij}^M are shown in Appendix A. By solving the integral in (13), one will get the time-domain response in a VTI medium.

Up to this step, we have not used an approximation. However, the

integral over horizontal slowness in (13) cannot be solved analytically in general VTI media. The asymptotic solution of (13) can be found with the stationary phase approximation, which yields the numerical calculation of the stationary-phase points (Appendix D). However, due to the complicated nature of VTI media, there is still no general analytical way of finding the stationary-phase points (which are the horizontal slowness in the present problem) for P-SV coupled Green's tensor.

SH-WAVE GREEN'S TENSOR

The SH-wave Green's tensor is in presence of G_{11}, G_{12}, and G_{22}. Since the vertical slowness of the SH-wave is always elliptical [eq. (12)], the asymptotic solution can be found by standard stationary phase approximation. The calculated stationary-phase point is shown in (14)

$$p_r^{\gamma} = (1/V_{S0})\{r^2/[(C_{66}/C_{44})r^2 + (C_{66}^2/C_{44}^2)|z|^2]\}^{1/2} \quad , \tag{14}$$

while the SH-wave Green's tensor is shown in Appendix B. Eq. (14) reflects the velocity anisotropy that the stationary-phase point generally does not corresponding to the phase slowness in the direction that connects the source and the observation point. Such property will force the radiation patterns to be deviated from the isotropic case, where the amplitude is only related to the projection of the source.

GREEN'S TENSOR IN WEAK-TI MEDIA

In this section, the Green's tensor in weak VTI media is being discussed. First of all, the method of approximation is introduced. Secondly, the error brought by the approximation is discussed. Finally, the radiation patterns calculated by the approximate solution are compared with the numerically computed asymptotic solution.

The vertical slowness of P- and SV-wave in (12) can be expanded into Taylor series to the first-order of Thomsen parameters δ and ε. The results are shown in (15)

$$\begin{aligned} p_{\alpha,w}^2 &= (1/V_{P0}^2) - (1 + 2\delta)p_r^2 + 2p_r^4V_{P0}^2(\delta - \varepsilon) \quad , \\ p_{\beta,w}^2 &= (1/V_{S0}^2) - (1 + 2\sigma)p_r^2 - 2p_r^4V_{P0}^2(\delta - \varepsilon) \quad , \\ \sigma &= (\delta - \varepsilon)/(f - 1) \quad , \end{aligned} \tag{15}$$

where σ is the combined parameter which controls the behavior of SV-wave

(Tsvankin and Thomsen, 1994). Although the linearization is based on individual anisotropic parameters, the high-order terms in (15) are depending on the difference between ε and δ. When $\varepsilon = \delta$, eq. (15) will become the exact formula for elliptical anisotropy (Ben-Menahem and Sena, 1990).

To this point, it seems that the term weak-TI is not appropriate since the approximation in (15) is not limited to the magnitude of each individual Thomsen parameter but the difference $\delta - \varepsilon$. However, when the degree of anisotropy is increasing, the behavior of the SV-wave becomes more complicated (Tsvankin, 1995; Tsvankin, 2001). In this case, the Thomsen parameters are too big for approximating the anisotropic behavior of the SV-wave (Thomsen and Dellinger, 2003). As the cusps of the SV-wave wavefront are emerging (shear-wave triplication) in strong VTI media, the stationary-phase approximation is not appropriate for computing the asymptotic solution (Tsvankin, 1995). In the case of shear-wave triplication, the asymptotic solutions will still correspond to the correct ray direction but the amplitude will not be computed properly. So we will limit the approximate solution to weak-TI media in the present paper.

By incorporating (15), the cubic equations of the stationary-phase points $p_r^{w\alpha}$ (P-wave) and $p_r^{w\beta}$ (SV-wave) can be found in (16)

$$
\begin{aligned}
&16(z^2/r^2)V_{P0}^4(\delta - \varepsilon)^2(p_r^{w\alpha})^6 - [8(z^2/r^2)(1 + 2\delta) + 2](\delta - \varepsilon)V_{P0}^2(p_r^{w\alpha})^4 \\
&+ [(z^2/r^2)(1 + 2\delta)^2 + (1 + 2\delta)(p_r^{w\alpha})^2 - (1/V_{P0}^2) = 0 \quad , \\
&16(z^2/r^2)V_{P0}^4(\delta - \varepsilon)^2(p_r^{w\beta})^6 + [8(z^2/r^2)(1 + 2\sigma) + 2](\delta - \varepsilon)V_{P0}^2(p_r^{w\beta})^4 \\
&+ [(z^2/r^2)(1 + 2\sigma)^2 + (1 + 2\sigma)(p_r^{w\beta})^2 - (1/V_{S0}^2) = 0 \quad ,
\end{aligned}
\tag{16}
$$

where the similarity between these two equations can be noticed immediately. The stationary-phase points can be found analytically by solving (16). Among the three solutions of the cubic equation, only the one with real value has physical meaning. When $r = 0$ (corresponding to vertical propagation), the stationary-phase points of the horizontal slowness have to be set to zero to obtain a physically sounding solution. When $z = 0$, (16) reduce to quadratic eqs. (17)

$$
\begin{aligned}
&2(\delta - \varepsilon)V_{P0}^2(p_r^{w\alpha})^4 + (1 + 2\delta)(p_r^{w\alpha})^2 - (1/V_{P0}^2) = 0 \quad , \\
&(\delta - \varepsilon)V_{P0}^2(p_r^{w\beta})^4 + (1 + 2\sigma)(p_r^{w\beta})^2 - (1/V_{S0}^2) = 0 \quad ,
\end{aligned}
\tag{17}
$$

which is equivalent to (15) for the cases when waves only propagate horizontally. After finding the stationary-phase points, the asymptotic Green's tensor in weak-TI media can be found and they are listed in Appendix C.

As can be seen from (C-1) to (C-6), the asymptotic Green's tensor is also closely related to the second-derivative of the phase function ϕ''_α and ϕ''_β, for P- and SV-wave respectively. Similar to the dispersion relationship (15), ϕ''_α and ϕ''_β have an elliptical part, which is proportional to $(1+2\delta)/V_{P0}^2$ or $(1+2\sigma)/V_{S0}^2$, as well as several non-elliptical parts that are related with either $(\delta-\varepsilon)$ or $(\delta-\varepsilon)^2$. When the difference between δ and ε is small, the elliptical part will dominate the solution. As the difference $(\delta-\varepsilon)$ is increasing, the non-elliptical terms will make the Green's tensor becoming more complicated since these terms are weighted by the horizontal slowness.

In the present paper, the asymptotic radiation patterns are defined as the displacement at the unit distance (one kilometer) generated by the unit body force. The asymptotic radiation patterns of G_{33} at several polar angles are calculated by the weak-TI and ray solution then compared to the numerically computed Green's tensor for five models. The benchmarking numerical solution (Appendix D) is computed by the stationary-phase approximation but (12) is being used to compute the stationary-phase points, without involving any approximation of medium property. The ray Green's tensor is computed by the approximate solution in weak-TI media from Vavrycuk (1997).

The detailed parameters of elastic constants, density, and Thomsen parameters are listed in Table 1. The elastic constant C_{13} is chosen to make each model has a distinct value of σ. The radiation patterns are shown in Figs. 1 to 5 for the five models, respectively.

Table 1. Elastic constants (in GPa), density (in g/cm^3), and Thomsen parameters of five models being used in radiation patterns calculation.

Model	C11	C33	C13	C44	C66	ρ	δ	ε	σ
1	30	18	10	6	9	2.5	0.2593	0.3333	0.2222
2	30	18	10.5	6	9	2.5	0.3756	0.3333	0.1094
3	30	18	11	6	9	2.5	0.3356	0.3333	−0.0069
4	30	18	11.5	6	9	2.5	0.3756	0.3333	−0.1267
5	30	18	12	6	9	2.5	0.4167	0.3333	−0.2500

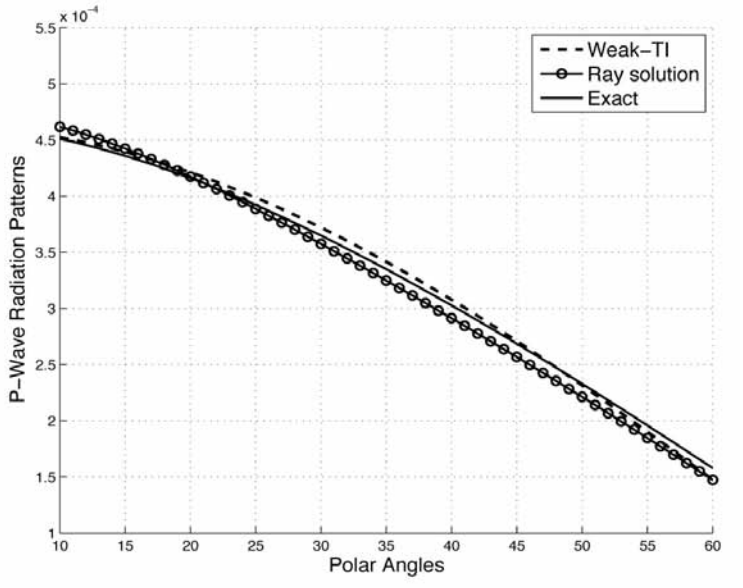

(a)

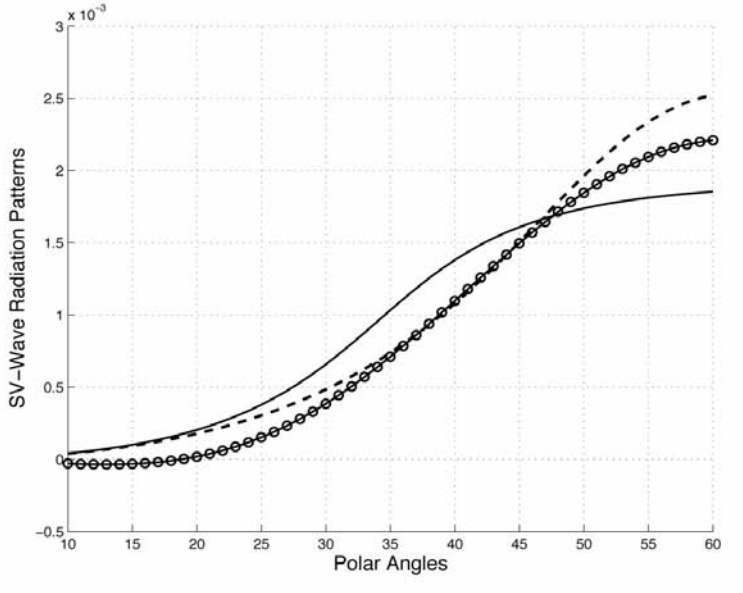

(b)

Fig. 1. (a) P-wave radiation patterns of G_{33} of model 1 calculated by weak-TI approximation (dashed line), ray approximation (circled line), and numerical method (solid line). (b) SV-wave radiation patterns of G_{33} of model 1 calculated by weak-TI approximation (dashed line), ray approximation (circled line), and numerical method (solid line).

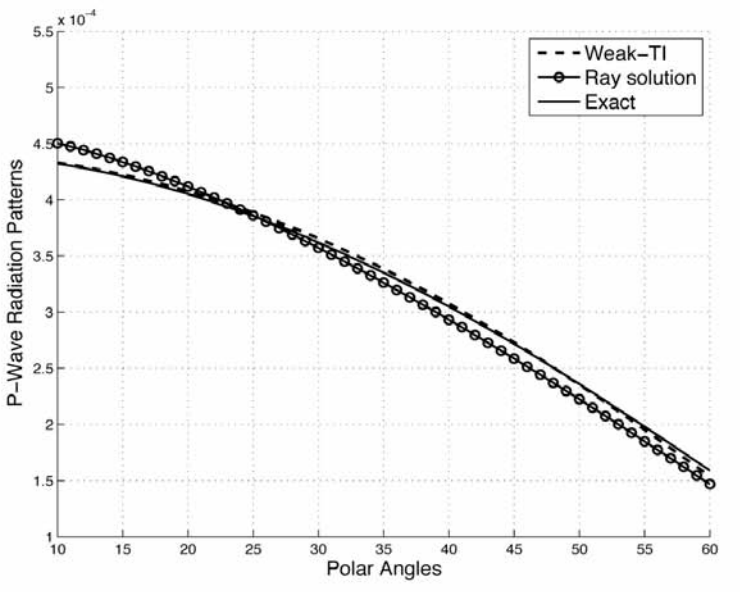

Fig. 2. (a) P-wave radiation patterns of G_{33} of model 2 calculated by weak-TI approximation (dashed line), ray approximation (circled line), and numerical method (solid line). (b) SV-wave radiation patterns of G_{33} of model 2 calculated by weak-TI approximation (dashed line), ray approximation (circled line), and numerical method (solid line).

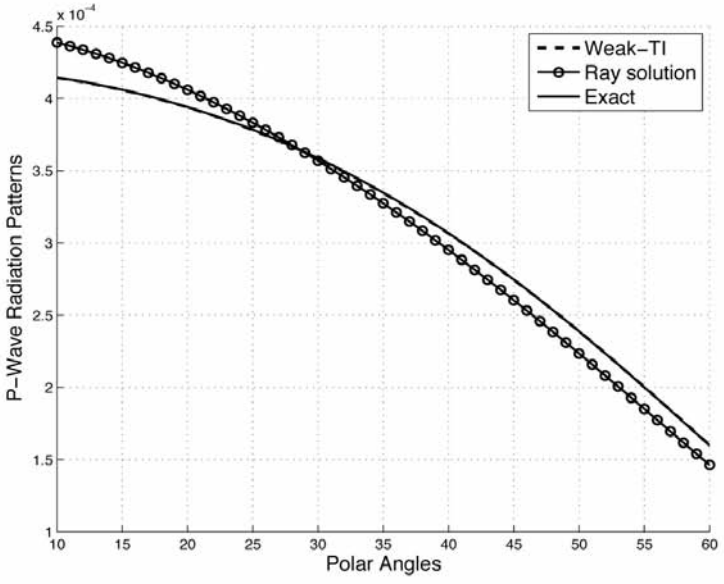

(a)

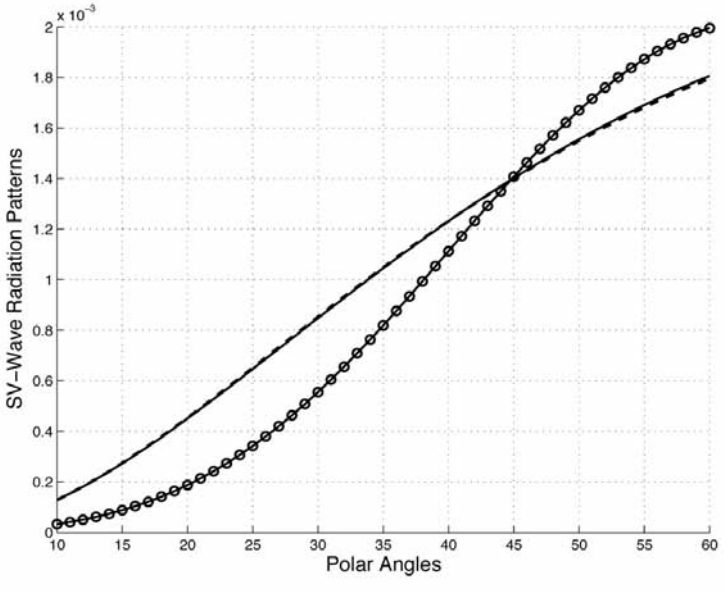

(b)

Fig. 3. (a) P-wave radiation patterns of G_{33} of model 3 calculated by weak-TI approximation (dashed line), ray approximation (circled line), and numerical method (solid line). (b): SV-wave radiation patterns of G_{33} of model 3 calculated by weak-TI approximation (dashed line), ray approximation (circled line), and numerical method (solid line).

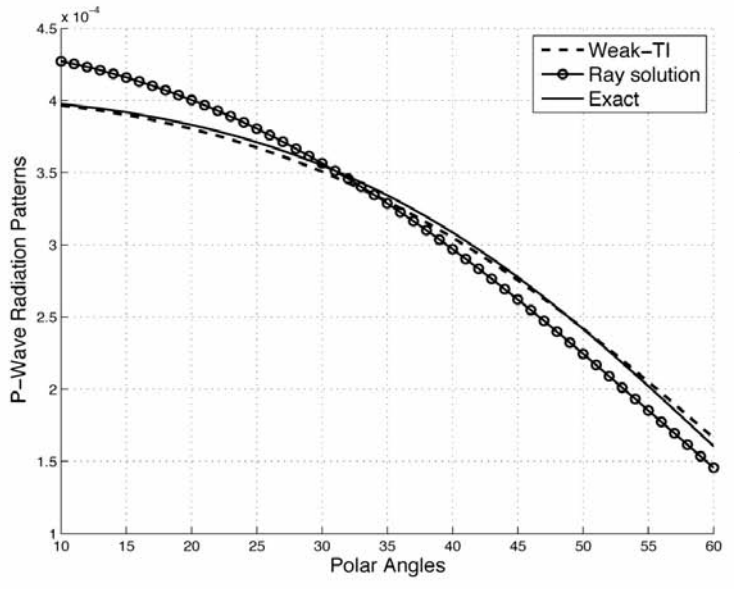

Fig. 4. (a) P-wave radiation patterns of G_{33} of model 4 calculated by weak-TI approximation (dashed line), ray approximation (circled line), and numerical method (solid line). (b): SV-wave radiation patterns of G_{33} of model 4 calculated by calculated by weak-TI approximation (dashed line), ray approximation (circled line), and numerical method (solid line).

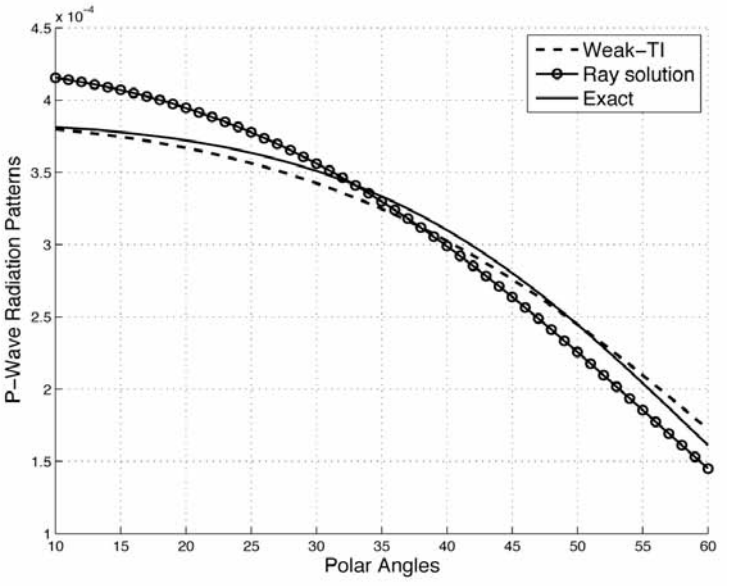

(a)

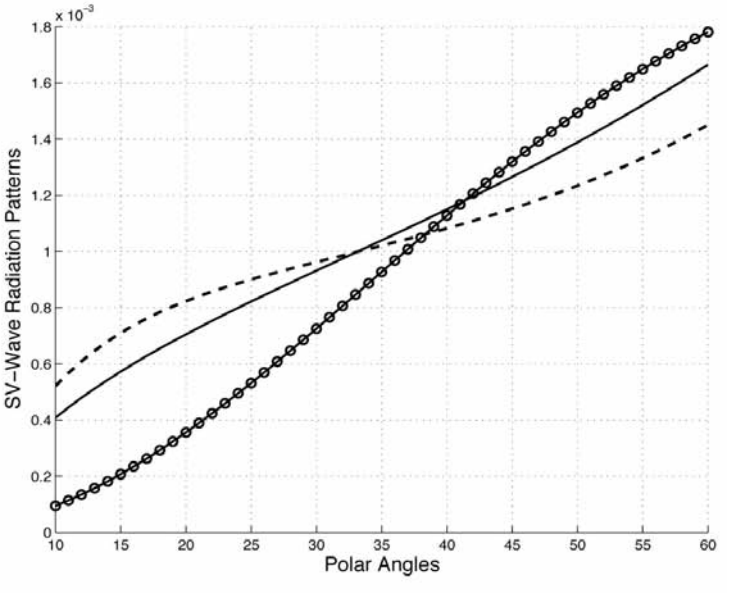

(b)

Fig. 5. (a) P-wave radiation patterns of G_{33} of model 5 calculated by weak-TI approximation (dashed line), ray approximation (circled line), and numerical method (solid line). (b): SV-wave radiation patterns of G_{33} of model 5 calculated by weak-TI approximation (dashed line), ray approximation (circled line), and numerical method (solid line).

As can be seen from Fig. 3 (a) and (b), the weak-TI solutions are almost identical to the benchmarks due to the small value of σ. For other models, weak-TI results are deviated from numerical solutions. The reason is (15), which is only to the fourth power of horizontal slowness p_r, is being used to approximate (12), which has a much more complicated relationship toward p_r. Thus whether or not (15) is close to (12) will strongly influence the weak-TI result. The approximate P-wave radiation patterns are closer to numerical solutions than SV-waves. One reason is that the vertical slowness of a P-wave is smaller than a SV-wave in nature. Thus the deviation of (15) from (12) will have a less significant effect on the P-wave. As mentioned above, another reason is that the physical nature of the SV-wave is much more complicated than that of the P-wave. The weak-TI solutions are generally closer to benchmarks than ray solutions. This is partly due to the methodology. While the current approximation is based on expanding the vertical slowness, the ray solution is computed by perturbation theorem, which leads to the radiation patterns is linearized in terms of the anisotropic parameters.

We will now focus on SV-wave radiation patterns from weak-TI solution. Comparing Figs. 1 and 2 to 4 and 5, it can be seen that the different sign of σ will lead the weak-TI solution to behave differently. When $\sigma > 0$, from Fig. 1 (b) and 2 (b), the approximate radiation patterns are not far away from the numerical solutions within a relatively small polar angle. After that, they deviate from the benchmarks much faster [Fig. 1 (b)]. When $\sigma > 0$, the situation is reversed. As can be seen from Fig. 4 (b) and 5 (b), the slope of the approximate solution changes much quicker than the numerical solution. This is due to the structure of (18), when the sign of σ reversed, the term related with the fourth power of the stationary-phase points will change sign thus leading to different behavior of stationary-phase points and radiation patterns. Previous studies (Thomsen, 1986; Tsvankin and Thomsen, 1994) indicate the positive value of σ to be predominant among different materials. Thus, we can often limit the approximate solution to small polar angles (less than 40 degrees) to get reliable approximations.

CONCLUSION

The impulse response in a VTI medium is evaluated in the asymptotic region analytically, while the full solution can be written as an inverse Hankel transform. The asymptotic SH-wave Green's tensor is found in general VTI medium. An approximate Green's tensor in weak-TI media is derived by expanding the vertical slowness into linear terms of Thomsen parameters where the stationary-phase points can be found analytically as well. Such solution is consistent with the analytic result obtained when $\varepsilon = \delta$. The weak-TI solution reflected the physical nature of VTI media and confirmed the previous understanding of anisotropic parameters (Tsvankin and Thomsen, 1994). The

approximate P-wave radiation patterns are generally more accurate than the SV-wave. Such observation has resulted from the simpler physical nature of the P-wave as well as the smaller absolute value of P-wave slowness. The accuracy of the approximate SV-wave solution is depending upon the anisotropic parameter σ. The sign of σ will influence the shape of the approximated solution. For the larger positive value of σ, the SV-wave radiation pattern will deviate from the true solution at large polar angles (over 40 degrees). While for the negative σ, the behavior of the approximate solution will have smaller deviation but the trend of deviation is more complicated.

ACKNOWLEDGEMENT

The authors would like to thank Ilya Tsvankin for reviewing the manuscript and providing insightful suggestions.

REFERENCES

Ben-Menahem, A. and Sena, A.G., 1990. Seismic source theory in stratified anisotropic media. J. Geophys. Res., 95: 15395-15427. doi: 10.1029/JB095iB10p15395.

Dellinger, J.A., 1991. Anisotropic Seismic Wave Propagation. Ph.D. Thesis, Department of Geophysics, Stanford University, Stanford, CA.

Fuchs, K. and Müller, G., 1971. Computation of synthetic seismograms with the reflectivity method and comparison with observations. Geophys. J., 23: 417. doi: 10.1111/j.1365-246X.1971.tb01834.x.

Gajewski, D., 1993. Radiation from point sources in general anisotropic media. Geophys. J. Internat., 113: 299-317. doi: 10.1111/j.1365-246X.1993.tb00889.x.

Gridin, D., 2000. Far-field asymptotics of the Green tensor for a transversely isotropic solid. Proc. Roy. Soc., A 456: 571-591. doi: 10.1098/rspa.2001.0844.

Hung, S. and Forsyth, D.W., 1998. Modelling anisotropic wave propagation in oceanic inhomogeneous structures using the parallel multidomain pseudo-spectral method. Geophys. J. Internat., 133: 726-740. doi: 10.1046/j.1365-246X.1998.00526.x.

Kennett, B.L.N., 1983. Seismic Wave Propagation in Stratified Media. Cambridge University Press, Cambridge, UK.

Müller, G., 1985. The reflectivity method: a tutorial. J. Geophys., 58: 153-174.

Thomsen, L., 1986. Weak elastic anisotropy. Geophysics, 51: 1954-1966. doi:10.1190/1.1442051.

Thomsen, L. and Dellinger, J., 2003. On shear-wave triplication in polar-anisotropic media. J. Appl. Geophys., 54: 289-296. doi:10.1016/j.jappgeo.2003.08.008.

Tsvankin, I.D. and Chesnokov, E.M., 1990. Synthesis of body wave seismograms from point sources in anisotropic media. J. Geophys. Res., 95 (B7): 11317-11331. doi:10.1029/JB095iB07p11317.

Tsvankin, I. and Thomsen, L., 1994. Nonhyperbolic reflection moveout in anisotropic media. Geophysics, 59: 1290-1304. doi:10.1190/1.1443686.

Tsvankin, I., 1995. Body-wave radiation patterns and AVO in transversely isotropic media. Geophysics, 60: 1409-1425. doi:10.1190/1.1443876.

Tsvankin, I., 2001. Seismic Signatures and Analysis of Reflection Data in Anisotropic Media. Elsevier Science Publishers, Oxford.

Vavryčuk, V., and Yomogida, K., 1996. SH-wave Green tensor for homogeneous transversely isotropic media by higher-order approximations in asymptotic ray theory. Wave Motion, 23: 83-93.

Vavryčuk, V., 1997. Elastodynamic and elastostatic Green tensors for homogeneous weak transversely isotropic media. Geophys. J. Int., 130: 786-800. doi: 10.1111/j.1365-246X.1997.tb01873.x.

Vavryčuk, V., 2002. Asymptotic elastodynamic Green function in the kiss singularity in homogeneous anisotropic solids. Stud. Geophys. Geod., 46: 249-266. doi: 0.1023/A:1019854020095.

APPENDIX A

THE INTEGRAL REPRESENTATION OF GREEN'S TENSOR

The Green's tensor in the space-frequency domain can be represented by the integral over horizontal slowness. They are listed in (A-1) to (A-6):

$$T_1 = [(\rho - C_{44}p_r^2 - C_{33}p_\alpha^2)/p_\alpha(p_\alpha^2 - p_\beta^2)]e^{-i\omega p_\alpha|z|} - [(\rho - C_{44}p_r^2 - C_{33}p_\beta^2)/p_\beta(p_\alpha^2 - p_\beta^2)]e^{-i\omega p_\beta|z|} \quad ,$$

$$\begin{aligned} G_{11}(r,t) &= [i/2(2\pi)^2](1/C_{33}C_{44}) \\ &\times \int_{-\infty}^{\infty} e^{i\omega t} \int_0^{\infty} (T_1/2)[J_0(\omega p_r r) - (\cos^2\alpha - \sin^2\alpha)J_2(\omega p_r r)]\omega p_r dp_r d\omega \\ &- [i/2(2\pi)^2 C_{44}] \\ &\times \int_{-\infty}^{\infty} e^{i\omega t} \int_0^{\infty} (e^{-i\omega p_\gamma|z|}/2p_\gamma)[J_0(\omega p_r r) + (\cos^2\alpha - \sin^2\alpha)J_2(\omega p_r r)]\omega p_r dp_r d\omega \quad , \end{aligned} \tag{A-1}$$

$$\begin{aligned} G_{12}(r,t) &= -[i/2(2\pi)^2](\cos\alpha\sin\alpha/C_{33}C_{44}) \\ &\times \int_{-\infty}^{\infty} e^{i\omega t} \int_0^{\infty} T_1 J_2(\omega p_r r)\omega p_r dp_r d\omega \\ &- [i\cos\alpha\sin\alpha/2(2\pi)^2 C_{44}] \int_{-\infty}^{\infty} e^{i\omega t} \int_0^{\infty} (e^{-i\omega p_\gamma|z|}/p_\gamma)J_2(\omega p_r r)\omega p_r dp_r d\omega \quad , \end{aligned} \tag{A-2}$$

$$\begin{aligned} G_{13}(r,t) &= [i(C_{13}+C_{14})/2(2\pi)^2][\mathrm{sgn}(z)\cos\alpha/C_{33}C_{44})] \\ &\times \int_{-\infty}^{\infty} e^{i\omega t} \int_0^{\infty} [\{p_r p_\alpha/(p_\alpha^2 - p_\beta^2)\}e^{-i\omega p_\alpha|z|} \\ &- \{p_r p_\beta/(p_\alpha^2 - p_\beta^2)\}e^{-i\omega p_\beta|z|}]J_1(\omega p_r r)\omega p_r dp_r d\omega \quad , \end{aligned} \tag{A-3}$$

$$G_{22}(r,t) = [i/2(2\pi)^2](1/C_{33}C_{44})$$
$$\times \int_{-\infty}^{\infty} e^{i\omega t} \int_{0}^{\infty} (T_1/2)[J_0(\omega p_r r) + (\cos^2\alpha - \sin^2\alpha)J_2(\omega p_r r)]\omega p_r dp_r d\omega \qquad (A\text{-}4)$$
$$- [i/2(2\pi)^2 C_{44}]$$
$$\times \int_{-\infty}^{\infty} e^{i\omega t} \int_{0}^{\infty} (e^{-i\omega p_\gamma |z|}/2p_\gamma)[J_0(\omega p_r r) - (\cos^2\alpha - \sin^2\alpha)J_2(\omega p_r r)]\omega p_r dp_r d\omega \ ,$$

$$G_{23}(r,t) = [i(C_{13}+C_{14})/2(2\pi)^2][\mathrm{sgn}(z)\sin\alpha/C_{33}C_{44})]$$
$$\times \int_{-\infty}^{\infty} e^{i\omega t} \int_{0}^{\infty} [\{p_r p_\alpha/(p_\alpha^2 - p_\beta^2)\}e^{-i\omega p_\alpha |z|} \qquad (A\text{-}5)$$
$$- \{p_r p_\beta/(p_\alpha^2 - p_\beta^2)\}e^{-i\omega p_\beta |z|}]J_1(\omega p_r r)\omega p_r dp_r d\omega \ ,$$

$$G_{33}(r,t) = [i/2(2\pi)^2](1/C_{33}C_{44})$$
$$\times \int_{-\infty}^{\infty} e^{i\omega t} \int_{0}^{\infty} [\{(\rho - C_{11}p_r^2 - C_{44}p_\alpha^2)/p_\alpha(p_\alpha^2 - p_\beta^2)\}e^{-i\omega p_\alpha |z|} \qquad (A\text{-}6)$$
$$- \{(\rho - C_{11}p_r^2 - C_{44}p_\beta^2)/p_\beta(p_\alpha^2 - p_\beta^2)\}e^{-i\omega p_\beta |z|}]J_0(\omega p_r r)\omega p_r dp_r d\omega \ .$$

APPENDIX B

SH-WAVE GREEN'S TENSOR

The asymptotic SH-wave Green's tensor in VTI media can always be solved by stationary phase approximation. They are listed in (B-1) to (B-3):

$$G_{11}^{SH}(r,t) = [\sin^2\alpha/2(2\pi)^2][(1/\rho C_{66})(p_{\gamma,s}p_r^\gamma/r|z|)]^{1/2}$$
$$\times \int_{-\infty}^{\infty} e^{i\omega[t - p_r^\gamma r - p_{\gamma,s}|z|]}\, d\omega \ , \qquad (B\text{-}1)$$

$$G_{12}^{SH}(r,t) = -[\sin\alpha\cos\alpha/2(2\pi)^2][(1/\rho C_{66})(p_{\gamma,s}p_r^\gamma/r|z|)]^{1/2}$$
$$\times \int_{-\infty}^{\infty} e^{i\omega[t - p_r^\gamma r - p_{\gamma,s}|z|]}\, d\omega \ , \qquad (B\text{-}2)$$

$$G_{22}^{SH}(r,t) = [\cos^2\alpha/2(2\pi)^2][(1/\rho C_{66})(p_{\gamma,s}p_r^{\gamma}/r|z|)]^{1/2} \times \int_{-\infty}^{\infty} e^{i\omega[t-p_r^{\gamma}r-p_{\gamma,s}|z|]}\, d\omega \quad , \tag{B-3}$$

where p_r^{γ} is the stationary horizontal slowness and $p_{\gamma,s}$ is the vertical stationary slowness, which is shown in (B-4):

$$\begin{aligned} p_{\gamma,s} &= \sqrt{\{(1/V_{S0}^2) - (C_{66}/C_{44})(p_r^{\gamma})^2\}} \\ &= (1/V_{S0})\{1 - r^2/[r^2 + (C_{66}/C_{44})|z|^2]\}^{1/2} \quad . \end{aligned} \tag{B-4}$$

APPENDIX C

ASYMPTOTIC GREEN'S TENSOR IN WEAK VTI MEDIA

The approximated asymptotic Green's tensor are listed in (C-1) to (C-6):

$$T_2 = -[\rho - C_{44}(p_r^{w\alpha})^2 - C_{33}p_{\alpha,w\alpha}^2]/(p_{\alpha,w\alpha}^2 - p_{\beta,w\alpha}^2) \quad ,$$

$$T_3 = [\rho - C_{44}(p_r^{w\beta})^2 - C_{33}p_{\alpha,w\alpha}^2]/(p_{\alpha,w\beta}^2 - p_{\beta,w\beta}^2) \quad ,$$

$$\begin{aligned} G_{11}(r,t) &= [1/2(2\pi)^2](\cos^2\alpha/C_{33}C_{44})[(T_2p_r^{w\alpha}/p_{\alpha,w\alpha})\sqrt{(1/p_r^{w\alpha}r|z\|\phi_{\alpha}''|)} \\ &\times \int_{-\infty}^{\infty} e^{i\omega(t-p_{\alpha,w\alpha}|z|-p_r^{w\alpha}r)}d\omega \end{aligned} \tag{C-1}$$

$$+ (T_3p_r^{w\beta}/p_{\beta,w\beta})\sqrt{(1/p_r^{w\beta}r|z\|\phi_{\beta}''|)} \int_{-\infty}^{\infty} e^{i\omega(t-p_{\beta,w\beta}|z|-p_r^{w\beta}r)}d\omega] + G_{11}^{SH}(r,t) \quad ,$$

$$\begin{aligned} G_{12}(r,t) &= [1/2(2\pi)^2](\sin\alpha\cos\alpha/C_{33}C_{44})[(T_2p_r^{w\alpha}/p_{\alpha,w\alpha})\sqrt{(1/p_r^{w\alpha}r|z\|\phi_{\alpha}''|)} \\ &\times \int_{-\infty}^{\infty} e^{i\omega(t-p_{\alpha,w\alpha}|z|-p_r^{w\alpha}r)}\, d\omega \end{aligned} \tag{C-2}$$

$$+ (T_3p_r^{w\beta}/p_{\beta,w\beta})\sqrt{(1/p_r^{w\beta}r|z\|\phi_{\beta}''|)} \int_{-\infty}^{\infty} e^{i\omega(t-p_{\beta,w\beta}|z|-p_r^{w\beta}r)}\, d\omega] + G_{12}^{SH}(r,t) \quad ,$$

$$G_{22}(r,t) = [1/2(2\pi)^2](\sin^2\alpha/C_{33}C_{44})[(T_2 p_r^{w\alpha}/p_{\alpha,w\alpha})\sqrt{(1/p_r^{w\alpha} r\,|\,z\,\|\,\phi''_\alpha\,|\,)}$$

$$\times \int_{-\infty}^{\infty} e^{i\omega(t-p_{\alpha,w\alpha}|z|-p_r^{w\alpha}r)}\,d\omega$$

$$+ (T_3 p_r^{w\beta}/p_{\beta,w\beta})\sqrt{(1/p_r^{w\beta} r\,|\,z\,\|\,\phi''_\beta\,|\,)} \int_{-\infty}^{\infty} e^{i\omega(t-p_{\beta,w\beta}|z|-p_r^{w\beta}r)}d\omega] + G_{12}^{SH}(r,t) \quad , \tag{C-3}$$

$$G_{13}(r,t) = [(C_{13}+C_{44})/2(2\pi)^2][\mathrm{sgn}(z)\cos\alpha/C_{33}C_{44}]\{[-(p_r^{w\alpha})^2/(p_{\alpha,w\alpha}^2-p_{\beta,w\alpha}^2)]$$

$$\times \sqrt{(1/p_r^{w\alpha} r\,|\,z\,\|\,\phi''_\alpha\,|\,)} \int_{-\infty}^{\infty} e^{i(\omega t-p_{\alpha,s\alpha}|z|-p_r^{\alpha}r)}\,d\omega$$

$$+ [(p_r^{w\beta})^2/(p_{\alpha,w\beta}^2-p_{\beta,w\beta}^2)]\sqrt{(1/p_r^{w\beta} r\,|\,z\,\|\,\phi''_\beta\,|\,)} \int_{-\infty}^{\infty} e^{i(\omega t-p_{\beta,s\beta}|z|-p_r^{\beta}r)}\,d\omega\} \quad , \tag{C-4}$$

$$G_{23}(r,t) = [(C_{13}+C_{44})/2(2\pi)^2][\mathrm{sgn}(z)\sin\alpha/C_{33}C_{44}]\{[-(p_r^{w\alpha})^2/(p_{\alpha,w\alpha}^2-p_{\beta,w\alpha}^2)]$$

$$\times \sqrt{(1/p_r^{w\alpha} r\,|\,z\,\|\,\phi''_\alpha\,|\,)} \int_{-\infty}^{\infty} e^{i(\omega t-p_{\alpha,s\alpha}|z|-p_r^{\alpha}r)}\,d\omega$$

$$+ [(p_r^{w\beta})^2/(p_{\alpha,w\beta}^2-p_{\beta,w\beta}^2)]\sqrt{(1/p_r^{w\beta} r\,|\,z\,\|\,\phi''_\beta\,|\,)} \int_{-\infty}^{\infty} e^{i(\omega t-p_{\beta,s\beta}|z|-p_r^{\beta}r)}\,d\omega\} \quad , \tag{C-5}$$

$$G_{33}(r,t) = [1/2(2\pi)^2](1/C_{33}C_{44})[-\{[\rho-C_{11}(p_r^{w\alpha})^2-C_{44}p_{\alpha,w\alpha}^2]/(p_{\alpha,w\alpha}^2-p_{\beta,w\alpha}^2)\}$$

$$\times (p_r^{w\alpha}/p_{\alpha,w\alpha})\sqrt{(1/p_r^{w\alpha} r\,|\,z\,\|\,\phi''_\alpha\,|\,)} \int_{-\infty}^{\infty} e^{i\omega(t-p_{\alpha,w\alpha}|z|-p_r^{w\alpha}r)}d\omega$$

$$+ \{[\rho-C_{11}(p_r^{w\beta})^2-C_{44}p_{\beta,w\beta}^2]/(p_{\alpha,w\beta}^2-p_{\beta,w\beta}^2)\}(p_r^{w\beta}/p_{\beta,w\beta})$$

$$\times \sqrt{(1/p_r^{w\beta} r\,|\,z\,\|\,\phi''_\beta\,|\,)} \int_{-\infty}^{\infty} e^{i\omega(t-p_{\beta,w\beta}|z|-p_r^{w\beta}r)}d\omega] \quad , \tag{C-6}$$

where ϕ''_α and ϕ''_β are shown in (C-7):

$$\phi''_\alpha = (1/p_{\alpha,w\alpha}^3)\{[(1+2\delta)/V_{P0}^2] - 12(p_r^{w\alpha})^2(\delta-\varepsilon)$$

$$+ 6V_{P0}^2(p_r^{w\alpha})^4(1+2\delta)(\delta-\varepsilon) - 8V_{P0}^4(p_r^{w\alpha})^6(\delta-\varepsilon)^2\} \quad ,$$

$$\phi''_{\beta} = (1/p^3_{\beta,w\beta})\{[(1+2\sigma)/V^2_{S0}] + 12(C_{33}/C_{44})(p_r^{w\beta})^2(\delta-\varepsilon)$$

$$- 6V^2_{P0}(p_r^{w\beta})^4(1+2\sigma)(\delta-\varepsilon) - 8V^4_{P0}(p_r^{w\beta})^6(\delta-\varepsilon)^2\} \quad . \tag{C-7}$$

The stationary-phase points $p_r^{w\alpha}$ and $p_r^{w\beta}$ can be found by solving (18) while other variables are listed in (C-8):

$$\begin{aligned}
p^2_{\alpha,w\alpha} &= (1/V^2_{P0}) - (1+2\delta)(p_r^{w\alpha})^2 + 2(p_r^{w\alpha})^4V^2_{P0}(\delta-\varepsilon) \quad , \\
p^2_{\alpha,w\beta} &= (1/V^2_{P0}) - (1+2\delta)(p_r^{w\beta})^2 + 2(p_r^{w\beta})^4V^2_{P0}(\delta-\varepsilon) \quad , \\
p^2_{\beta,w\beta} &= (1/V^2_{S0}) - (1+2\sigma)(p_r^{w\beta})^2 - 2(p_r^{w\beta})^4V^2_{P0}(\delta-\varepsilon) \quad , \\
p^2_{\beta,w\alpha} &= (1/V^2_{S0}) - (1+2\sigma)(p_r^{w\alpha})^2 - 2(p_r^{w\alpha})^4V^2_{P0}(\delta-\varepsilon) \quad .
\end{aligned} \tag{C-8}$$

APPENDIX D

ASYMPTOTIC GREEN'S TENSOR

The asymptotic solution in general VTI media requires computing the stationary-phase points numerically. Such problem can be formulated as to minimize the absolute value of the first-derivative of the phase function. The first- and second-derivative of the vertical slowness is provided below:

$$\partial p_z/\partial p_r = (A/p_z)p_r + (\eta/2p_z)(\partial S/\partial p_r) \quad ,$$

$$\partial^2 p_z/\partial p_r^2 = -(A/p_z^2)p_r(\partial p_z/\partial p_r) + (A/p_z) + (\eta/2p_z)(\partial^2 S/\partial p_r^2)$$

$$- (\eta/2p_z^2)(\partial S/\partial p_r)(\partial p_z/\partial p_r) \quad ,$$

$$p_z = \sqrt{\{Ap_r^2 + B + \eta S\}} \quad , \quad S = [1/2(f-1)]\sqrt{\{A_1p_r^4 + B_1p_r^2 + C_1\}} \quad ,$$

$$\partial S/\partial p_r = (2A_1p_r^3 + B_1p_r)/2(f-1)\sqrt{\{A_1p_r^4 + B_1p_r^2 + C_1\}} \quad ,$$

$$\partial^2 S/\partial p_r^2 = [(6A_1p_r^2 + B_1)/2(f-1)\sqrt{(A_1p_r^4 + B_1p_r^2 + C_1)}]$$

$$- [(2A_1p_r^3 + B_1p_r)^2/2(f-1)(A_1p_r^4 + B_1p_r^2 + C_1)^{3/2}] \quad ,$$

$$A = (\varepsilon + 1 - f - f\delta)/(f-1) \quad , \quad B = (f-2)/2(f-1)V^2_{P0} \quad ,$$

$$A_1 = 4f^2[(\delta+1)^2 - 2\varepsilon - 1] + 8(\varepsilon - \delta - \varepsilon\delta)f + 4\varepsilon^2 \quad ,$$

$$B_1 = (8f\delta - 4f\varepsilon - 4f^2\delta)(1/V^2_{P0}) \quad , \quad C_1 = f^2/V^4_{P0} \quad , \tag{D-1}$$

where $\eta = 1$ for the P-wave and -1 for the SV-wave. The stationary-phase point can be found by inserting the above formula into the derivative of the phase function. Once the stationary-phase points are found, the corresponding vertical slowness can be calculated by (12) and the second derivative of the phase function is just $|z|\partial^2 p_z/\partial p_r^2$. Then the asymptotic Green's tensor is found by inserting these values into (C-1) to (C-6).